A unified Bayesian framework for relative microseismic location

Oleg V. Poliannikov,[1] Michael Prange,[2] Alison Malcolm[1] and Hugues Djikpesse[2]

[1]*Earth Resources Laboratory,* 54-521A, *MIT,* 77 *Massachusetts Ave., Cambridge,* MA 02139-4307, *USA. E-mail: poliann@mit.edu*
[2]*Schlumberger-Doll Research Center,* 1 *Hampshire St., Cambridge,* MA 02139-1578, *USA*

SUMMARY

We study the problem of determining an unknown microseismic event location relative to previously located events using a single monitoring array in a monitoring well. We show that using the available information about the previously located events for locating new events is advantageous compared to locating each event independently. By analysing confidence regions, we compare the performance of two previously proposed location methods, double-difference and interferometry, for varying signal-to-noise ratio and uncertainty in the velocity model. We show that one method may have an advantage over another depending on the experiment geometry, assumptions about uncertainty in velocity and recorded signal, etc. We propose a unified approach to relative event location that includes double-difference and interferometry as special cases, and is applicable to velocity models and well geometries of arbitrary complexity, producing location estimators that are superior to those of double-difference and interferometry.

Key words: Numerical solutions; Instability analysis; Interferometry; Computational seismology; Theoretical seismology.

1 INTRODUCTION

Locating seismic events is an important problem both in global seismology and in exploration. Applications of this problem vary in scale from earthquake characterization to hydraulic fracture monitoring. In hydraulic fracture monitoring, locating microseismic events is an indirect method to image fractures or monitor their growth (Michaud *et al.* 2004; Bennett *et al.* 2005; Huang *et al.* 2006).

Traditionally event location is performed as follows. For each event observed from a single well, its arrival time and polarization are estimated. Polarization can only be estimated with multi-component receivers, and it provides an indication of the direction of the arriving signal. Combining the measured traveltime and polarization with an assumed velocity model allows the recorded event to be, for instance, ray traced to its estimated location. Microseismic events are located one by one, and the location of one is not used to improve the estimated location of another.

As will be elaborated further, the classical location technique described above fails to use important information that couples data from different events, and that can be used to constrain the location of an unknown event relative to already located events (Dewey 1972; Fitch 1975; Spence 1980; Richards *et al.* 2006; Hulsey *et al.* 2009; Kummerow 2010). If multiple events originate in the same fracture then this relative location could contain useful information about the geometry of the fracture or its growth in time (Eisner *et al.* 2006). When multiple fractures are created sequentially, relative distances between the events from different fractures reveal important information about the geometry of the entire fracture system.

When one event is located relative to another, the uncertainty in the origin time and absolute location of the reference event propagates to the estimates of the origin time and the absolute location of the unknown event. However, estimating quantities such as the fracture size or fracture spacing does not require the knowledge of the absolute locations of the events. For example, we may hypothetically move the entire fracture system in space without changing the size of individual fractures or their relative arrangement. Relative location is a method of recovering quantities that are not sensitive to absolute event positions.

In this paper, we consider two methods of relative location that have been previously proposed: double-difference (DD) (Waldhauser & Ellsworth 2000; Zhang & Thurber 2003) and interferometry (Poliannikov *et al.* 2011). Both methods use correlations of waveform data around direct arrivals from different sources at multiple receivers, henceforth called correlograms, to couple the arrivals of pairs of events. These correlograms produce new measurements of wave propagation between the events that are less sensitive to the global variations of the velocity (Zhang & Thurber 2003; Borcea *et al.* 2005; Zhang & Thurber 2006).

GJI Seismology

While the rationale for using double-difference and interferometry is similar, the methods differ in important aspects. The double-difference location method seeks to match predicted correlograms with observed ones uniformly across all receivers, while the interferometric location method fits the correlogram only at a single stationary receiver where the correlation lag is maximal.

To compare the performance of each method, an objective measure is required. Such a measure can then be used to test each method for a range of realistic scenarios.

We consider here a numerical experiment with a single monitoring well and two fractures that are located near one another. Event locations in the first reference fracture are assumed known, and we attempt to locate an event in another fracture using all the information that is available. We assume that the velocities in the overburden are uncertain and that the recorded signal is noisy. Using these assumptions we define location estimators for both methods and compute the associated uncertainty. Analysis of the location uncertainty reveals the situations in which one method is superior to another.

The uncertainty analysis that we develop is general and applies to any relative location method that uses the fit between predicted correlograms and observed ones. Accordingly, instead of choosing between the two methods, we seek a correlogram-based location method that minimizes the location uncertainty given accepted assumptions on the signal noise and velocity uncertainty (Tarantola & Valette 1982; Pavlis 1986). Specifically, we seek the subset of receivers, which when used for relative location, minimizes the uncertainty of the estimate of the event location. The output of this procedure is the set of optimal receivers and the associated event location uncertainty. In some cases the optimal receivers will be nearly stationary. In other cases, it may be advantageous to use all or a subset of available receivers away from the stationary point. The search for optimal receivers is fully automated and by construction outperforms both double-difference and interferometry.

The structure of this paper is as follows. In Section 2, we discuss event location in a known velocity when event origin times are known. In Section 3, we introduce the notion of relative location in an unknown velocity, build a framework for evaluating the performance of different methods, and propose a unified relative location method. In Section 4, we generalize our methodology to events whose origin times are unknown. In Section 5, we present a set of 1- and 2-D examples that demonstrate the versatility of our methodology. The paper closes with a concluding section.

2 LOCATION IN A KNOWN VELOCITY

2.1 Classical location

A collection of seismic events excites elastic waves that are then recorded by a set of single-component or multiple-component receivers. The problem is to locate these events using the recorded signals. A classical method of event location is to locate each event individually. For each event, the arrival time of each recorded phase is picked at each receiver, and when combined with an assumed velocity model and event polarity information, ray tracing can be used to find the event location. Throughout the paper we consider a situation where the recorded signal is noisy, and thus the picked traveltimes are noisy. For clarity we first assume that the event origin times are known. In Section 4, we show that our approach fully extends to the case of unknown origin times.

Suppose that, for a given wave arrival, the picked (measured) traveltime, $\hat{T}_{\alpha,j}$, of phase α at receiver j can be written as

$$\hat{T}_{\alpha,j} = T_\alpha\left(\boldsymbol{s}, \boldsymbol{r}_j\right) + \varepsilon_{\alpha,j}, \quad \alpha = P, S, \ldots, \ j = 1, \ldots, N_\mathrm{r}, \tag{1}$$

where N_r is the number of receivers in the monitoring well, $T_P(\boldsymbol{s}, \boldsymbol{r}_j)$ and $T_S(\boldsymbol{s}, \boldsymbol{r}_j)$ are the predicted traveltime of the P and S wave from an event location $\boldsymbol{s}$ to a receiver location $\boldsymbol{r}_j$ computed by ray tracing in the assumed velocity model V_P or V_S, respectively; $\varepsilon_{\alpha,j}$ is independent Gaussian noise, given by $\varepsilon_{\alpha,j} \sim \mathcal{N}(0, \sigma_{\alpha,j}^2)$, that is, normally distributed with zero-mean and variance $\sigma_{\alpha,j}^2$. We may potentially use a richer set of phases α to distinguish between SH and SV or include other arrivals such as reflections from known interfaces if we can model them theoretically and they are present in the data. The method is also easily generalized to the case of correlated $\varepsilon_{\alpha,j}$ with a known covariance matrix. For now we will use the notation as it has been defined. The likelihood function for the observed traveltimes is given by Tarantola & Valette (1982) and Eisner *et al.* (2010)

$$p_{\mathrm{CL}}\left(\{\hat{T}_{\alpha,j}\} \mid \boldsymbol{s}\right) = \frac{1}{(2\pi)^{N_\mathrm{r}/2} \prod\limits_{\alpha,j} \sigma_{\alpha,j}} \exp\left[-\frac{1}{2}\sum_{\alpha,j}\left(\frac{\hat{T}_{\alpha,j} - T_\alpha\left(\boldsymbol{s}, \boldsymbol{r}_j\right)}{\sigma_{\alpha,j}}\right)^2\right], \tag{2}$$

where CL stands for classical. The posterior distribution, $p_{\mathrm{CL}}(\boldsymbol{s} \mid \{\hat{T}_{\alpha,j}\})$, of the event location, $\boldsymbol{s}$, given the observed traveltimes, $\{\hat{T}_{\alpha,j}\}$, is obtained using Bayes' rule

$$p_{\mathrm{CL}}\left(\boldsymbol{s} \mid \{\hat{T}_{\alpha,j}\}\right) = \frac{p_{\mathrm{CL}}\left(\{\hat{T}_{\alpha,j}\} \mid \boldsymbol{s}\right) p(\boldsymbol{s})}{\iiint p_{\mathrm{CL}}\left(\{\hat{T}_{\alpha,j}\} \mid \boldsymbol{s}\right) p(\boldsymbol{s})\, d\boldsymbol{s}}, \tag{3}$$

where $p(s)$ is the prior probability density. Assuming a uniform prior probability $p(s) \equiv \text{const}$, we have

$$p_{\text{CL}}\left(s \mid \{\hat{T}_{\alpha,j}\}\right) \propto \exp\left[-\frac{1}{2}\sum_{\alpha,j}\left(\frac{\hat{T}_{\alpha,j} - T_{\alpha}\left(s, r_j\right)}{\sigma_{\alpha,j}}\right)^2\right]. \tag{4}$$

2.2 Reducing uncertainty by using correlograms

In practice, we may need to locate many seismic events. Waldhauser & Ellsworth (2000) have shown that instead of locating sources one by one we can use available information about previously located events to obtain better estimates of the locations of subsequent events.

Assume, for example, that we have already located N_s events: $s_1, \ldots, s_{N_s}$. The goal is to locate an unknown event s. To use information from the already located events, we use the original waveforms to compute cross-correlations of direct arrivals from events s_i with that from event s for each receiver. We obtain correlogram picks

$$\hat{\tau}_{\alpha,i,j} = \tau_{\alpha}\left(s_i, s, r_j\right) + \eta_{\alpha,i,j}, \tag{5}$$

where $\tau_{\alpha}(s_i, s, r_j)$ is the predicted correlogram moveout in the assumed velocity model V_{α}:

$$\tau_{\alpha}\left(s_i, s, r_j\right) = T_{\alpha}\left(s, r_j\right) - T_{\alpha}\left(s_i, r_j\right), \tag{6}$$

and $\eta_{\alpha,i,j}$ is independent Gaussian noise given by $\eta_{\alpha,i,j} \sim \mathcal{N}(0, \zeta_{\alpha,i,j}^2)$. Note that although the predicted correlogram event moveouts in eq. (6) are differences of the corresponding traveltimes in the original gathers, correlogram picks, $\hat{\tau}_{\alpha,i,j}$, are not simply differences of the traveltime picks; they are computed independently directly from the waveforms.

Assuming that the events $s_1, \ldots, s_{N_s}$ have already been located, we simultaneously fit the predicted traveltimes, $T_{\alpha}(s, r_j)$ to the observed time picks, $\hat{T}_{\alpha,j}$, and the predicted correlogram moveouts, $\tau_{\alpha}(s_i, s, r_j)$, to the observed lags, $\hat{\tau}_{\alpha,i,j}$. This allows us to calculate the conditional distribution of the unknown event location s given the previously located events. Since both the errors in the traveltimes and in the lags have Gaussian distributions, we can perform an analysis similar to the one in Section 2.1, and write the estimator of the location s given the observed traveltimes and lags as

$$p_{\text{DD}}\left(s \mid s_1, \ldots, s_{N_s}, \{\hat{T}_{\alpha,j}\}, \{\hat{\tau}_{\alpha,i,j}\}\right) \propto \exp\left[-\frac{1}{2}\sum_{\alpha,j}\left(\frac{\hat{T}_{\alpha,j} - T_{\alpha}\left(s, r_j\right)}{\sigma_{\alpha,j}}\right)^2\right] \times \exp\left[-\frac{1}{2}\sum_{i=1}^{N_s}\sum_{\alpha,j}\left(\frac{\hat{\tau}_{\alpha,i,j} - \tau_{\alpha}\left(s_i, s, r_j\right)}{\zeta_{\alpha,i,j}}\right)^2\right]. \tag{7}$$

Following Waldhauser & Ellsworth (2000) and Zhang & Thurber (2003), we call this location technique the double-difference method, so named due to the differencing of two residuals, $\hat{\tau}_{\alpha,i,j}$ and $\tau_{\alpha}(s_i, s, r_j)$, which are themselves differences of traveltimes. The classical method of direct event location given by eq. (4) processes each event independently, and thus fails to utilize the important constraints that couple pairs of events. Those constraints enter eq. (7) in the form of additional exponentials of lag misfits. This may result in a larger uncertainty in the classical location technique as compared to the double-difference method.

We illustrate the relative performance of the two methods in a numerical experiment with a layered velocity model and the source and receiver configuration shown in Fig. 1(a). The 16 receivers are equally spaced in a vertical well at depths between 1300 and 2900 m. The locations of the 25 events in the reference fracture, situated at an offset (horizontal distance) of 300 m, are assumed known. The unknown event is located further away at an offset of 600 m. The known layered velocity is shown in Figs 1(b) and (c).

In this initial demonstration we assume that the origin times of all events are known. Later, we show how to remove this assumption. The traveltimes, $\hat{T}_{\alpha,j}$, from the unknown event are picked with errors, and the standard deviation of these errors is $\sigma_{\alpha,j} \equiv 4\,\text{ms}$. The waveforms of the direct arrivals from the unknown event and the reference events are cross-correlated, and the lags are picked with the uncertainty $\zeta_{\alpha,i,j} \equiv 4\,\text{ms}$. We use eqs (4) and (7) to compute the conditional density of the location estimators given by the classical and double-difference methods. We use a fast eikonal solver to compute traveltimes from each of the 16 receivers. The likelihood function values, and hence the posterior distribution values, can then be efficiently computed throughout the 3-D volume. For this layered model, a two-point ray tracer might have been adequate. We use an eikonal solver because our methodology is appropriate for general 3-D models and our software is written for this general case.

Because the medium is layered and the well is vertical, both methods fail to recover the azimuth. The azimuthal information is available when the azimuthal symmetry of the model is broken, such as by a non-vertical well and/or a velocity model that is not horizontally stratified. Here, we will analyse the uncertainty in the offset-depth plane, where offset is horizontal distance between the receiver array and the event. The azimuth can be estimated by analysing the polarization of the incoming wave if three-component receivers are available. This issue is not relevant to the location algorithms discussed in this paper and we will not consider it any further.

We compare the performance of each method in Fig. 2. For each method we display the corresponding 95 per cent-confidence region. Both estimators are unbiased but the spread of the estimator constructed using the double-difference method is much smaller. This example shows how the use of already located events can improve the location accuracy of subsequently located events.
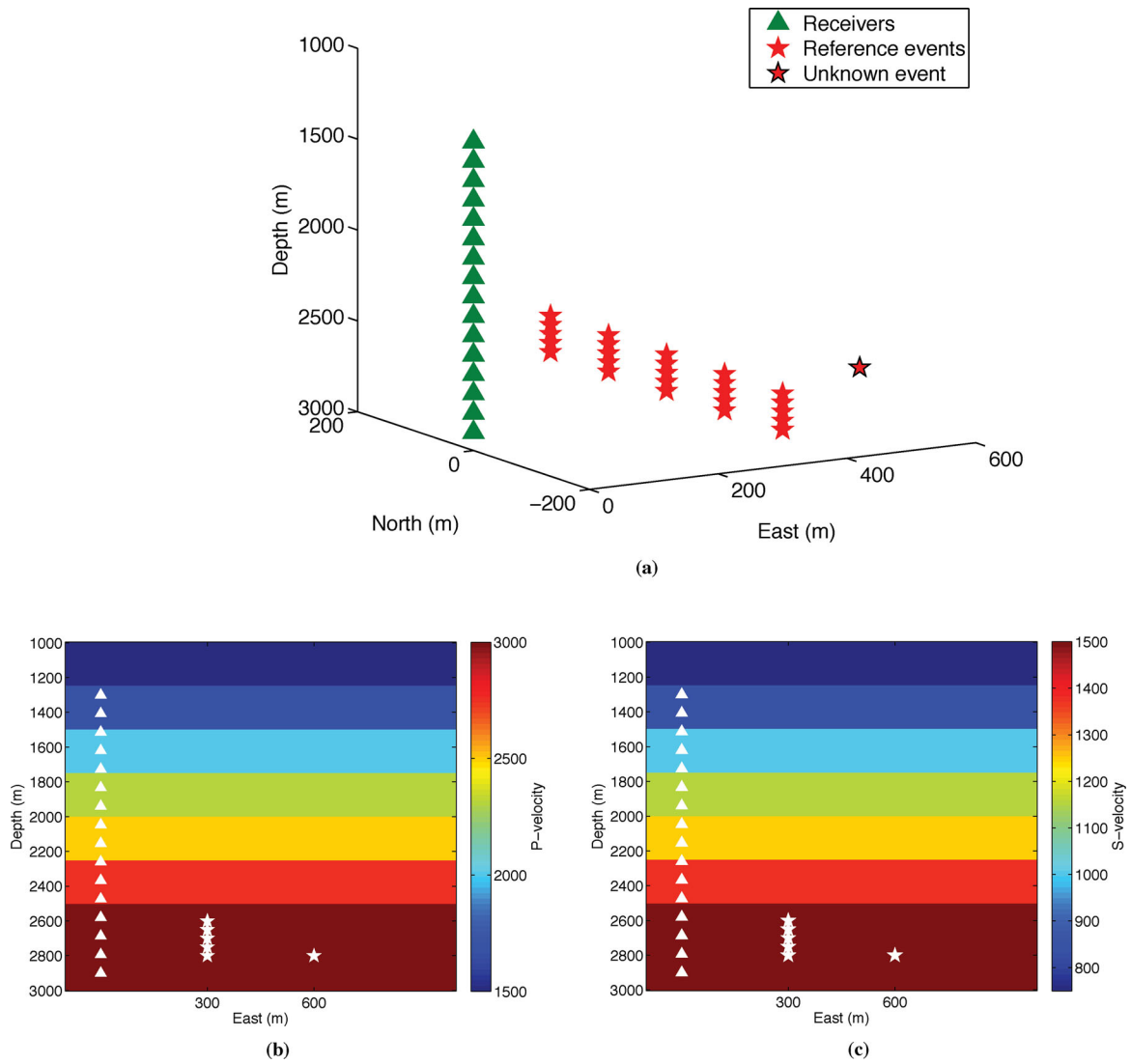
Figure 1. (a) The numerical setup with 16 receivers in a monitoring well located at depths from 1300 to 2900 m, 25 events in the reference fracture 300 m away from the well, and an unknown event in another fracture 600 m from the well; (b) The layered *P* velocity; (c) The layered *S* velocity.
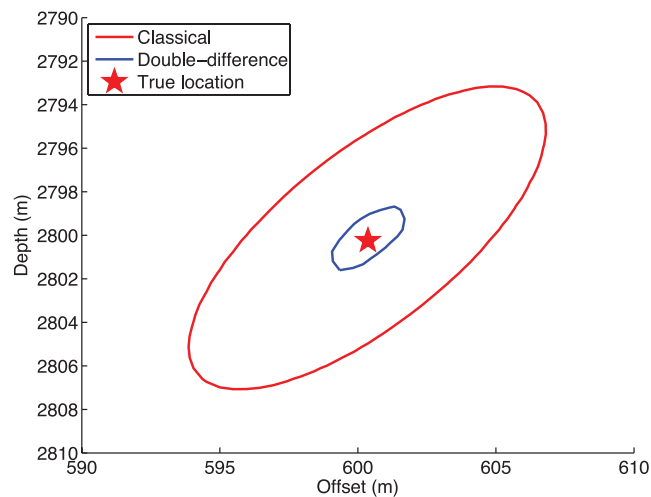

Figure 2. 95 per cent confidence regions for the layered velocity model with no velocity uncertainty.

3 LOCATION IN UNCERTAIN VELOCITY

3.1 Relative location

In the previous section, we have shown that if the velocity model is known, then the double-difference method provides a better estimate of the location of the unknown event than the classical method. Now we consider a scenario where the velocity model is uncertain. We denote the family comprising all admissible velocity models as $\mathscr{V}$.

The probability density functions given by eqs (4) and (7) implicitly depend on the assumed velocity model. If that velocity is incorrect, then the resulting estimators are based on erroneously predicted traveltimes and can be biased. In particular, the performance of the classical location method given by eq. (4) may significantly deteriorate. On the other hand, correlograms are less sensitive to the velocity uncertainty because cross-correlation in effect subtracts the traveltimes, and if the waves from two event locations travel to a receiver along similar paths, then the model uncertainty along the shared portion of the rays is largely cancelled. Our goal, as before, will be to estimate the location of the unknown event relative to previously located ones, and to analyse the resulting uncertainty due to both the noise in the signal and the uncertainty in the velocity model.

We emphasize the dependence of all computed traveltimes on the velocity model, $V \in \mathscr{V}$, by explicitly conditioning on the latter. The traveltimes and the correlogram lags will henceforth be denoted as $T_\alpha(s, r \mid V)$ and $\tau_\alpha(s_i, s, r \mid V)$. The conditional distribution of the unknown event location s is denoted $p(s \mid s_1, \ldots, s_{N_s}, \{\hat{T}_{\alpha,j}\}, \{\hat{\tau}_{\alpha,i,j}\}, V)$. Then the total uncertainty over all velocity models is described with the marginal distribution of s obtained by averaging properly normalized posterior distributions over all possible velocity models in $\mathscr{V}$

$$p\left(s \mid s_1, \ldots, s_{N_s}, \{\hat{T}_{\alpha,j}\}, \{\hat{\tau}_{\alpha,i,j}\}\right) = \sum_{V \in \mathscr{V}} p\left(s \mid s_1, \ldots, s_{N_s}, \{\hat{T}_{\alpha,j}\}, \{\hat{\tau}_{\alpha,i,j}\}, V\right) p(V). \tag{8}$$

If the velocity models are equally likely, then $p(V) = 1/|V|$, where $|V|$ is the cardinality of V. In what follows we consider two previously proposed methods for relative event location: the double-difference method and the interferometric method. We compare their relative performance in variouscenarios and analyse their strengths and weaknesses. This analysis will then form a basis for the new unified approach that combines the best of the two techniques and results in a location algorithm that outperforms either one.

3.2 Double-difference location

Because the velocity model is uncertain, the predicted traveltimes, $T_\alpha(s, r)$, are biased. For example, if the velocity is overestimated, then the event distance will have an overestimation bias. To partially mitigate this problem, we use only the correlogram lags to construct an estimate of the relative location of the unknown event:

$$p_{\text{DD}}(\{\hat{\tau}_{\alpha,i,j}\} \mid s, s_1, \ldots, s_{N_s}, V) \propto \exp\left[-\frac{1}{2} \sum_{i=1}^{N_s} \sum_{\alpha,j} \left(\frac{\hat{\tau}_{\alpha,i,j} - \tau_\alpha\left(s_i, s, r_j \mid V\right)}{\zeta_{\alpha,i,j}}\right)^2\right]. \tag{9}$$

The modified posterior distribution of the event location, conditional on the velocity model, is given by

$$p_{\text{DD}}(s \mid s_1, \ldots, s_{N_s}, \{\hat{\tau}_{\alpha,i,j}\}, V) \propto \frac{p_{\text{DD}}(\{\hat{\tau}_{\alpha,i,j}\} \mid s, s_1, \ldots, s_{N_s}, V)}{\iiint p_{\text{DD}}(\{\hat{\tau}_{\alpha,i,j}\} \mid s, s_1, \ldots, s_{N_s}, V) ds}. \tag{10}$$

Averaging over all possible velocity models, we obtain an estimate of the location of s relative to $s_1, \ldots, s_{N_s}$

$$p_{\text{DD}}(s \mid s_1, \ldots, s_{N_s}, \{\hat{\tau}_{\alpha,i,j}\}) = \sum_{V \in \mathscr{V}} p_{\text{DD}}(s \mid s_1, \ldots, s_{N_s}, \{\hat{\tau}_{\alpha,i,j}\}, V) p(V). \tag{11}$$

Using a large number of lag points significantly reduces the impact of signal noise. Because the correlograms are less sensitive to the velocity uncertainty between the receivers and the events, the estimator given in eq. (11) is less biased than the original double-difference estimator from eq. (7). However, the bias is not perfectly mitigated (Michelini & Lomax 2004), and to attempt to remove it more effectively we will construct in the next section a related estimator based on interferometry.

3.3 Interferometric location

The interferometric location method, proposed by Poliannikov *et al.* (2011), is another technique that can be employed to locate an unknown event relative to other events with known locations. Partially reconstructing the Green's function between the unknown event and the known event locations provides additional information that is complementary to that contained in the direct arrival times picked at the receivers. A summary of the method is as follows.

We first assume a velocity model, V, and perform a stationary phase analysis of the correlogram moveout. Specifically, for each reference event s_i, we take the observed lag moveout, $\hat{\tau}_{\alpha,i,j}$, interpolate it between the receivers as necessary, and find a stationary receiver location, $r_{\alpha,i,*}$, defined in our example with an observation well by

$$\partial_r \hat{\tau}_{\alpha,i,j} = 0, \tag{12}$$

where ∂_r denotes a directional derivative with respect to the receiver position along the well trajectory. (For a 2-D array of receivers, we would have to differentiate with respect to both spatial variables.) We interpolate the stationary location from the lag measurements and compute the stationary (maximum) lag

$$\hat{\tau}_{\alpha,i,*} = \hat{\tau}_{\alpha,i,j}\big|_{r_{\alpha,i,*}}. \tag{13}$$

As further elaborated by Poliannikov *et al.* (2011), $r_{\alpha,i,*}$ and $\hat{\tau}_{\alpha,i,*}$ may be used to constrain the location, s, of the unknown event relative to all other events, s_i, with which s forms stationary pairs. Their likelihood function is written as

$$p_{\mathrm{INT}}(\{r_{\alpha,i,*}, \hat{\tau}_{\alpha,i,*}\} \mid s, s_1, \ldots, s_{N_s}, V) \propto \exp\left[-\frac{1}{2}\sum_{i=1}^{N_s}\left(\frac{\hat{\tau}_{\alpha,i,*} - \tau_\alpha(s_i, s, r_{i,*} \mid V)}{\zeta_{\alpha,i,*}}\right)^2\right] \exp\left[-\frac{1}{2}\sum_{i=1}^{N_s}\left(\frac{\partial_r\tau_\alpha(s_i, s, r_{\alpha,i,*} \mid V)}{2\zeta_{\alpha,i,*}}\right)^2\right]. \tag{14}$$

The posterior distribution of the event location then has the form

$$p_{\mathrm{INT}}(s \mid s_1, \ldots, s_{N_s}, \{r_{i,*}, \hat{\tau}_{\alpha,i,*}\}, V) \propto \frac{p_{\mathrm{INT}}(\{r_{\alpha,i,*}, \hat{\tau}_{\alpha,i,*}\} \mid s, s_1, \ldots, s_{N_s}, V)}{\iiint p_{\mathrm{INT}}(\{r_{i,*}, \hat{\tau}_{\alpha,i,*}\} \mid s, s_1, \ldots, s_{N_s}, V)\,ds}. \tag{15}$$

Marginalizing over all possible velocity models, $V \in \mathcal{V}$, we obtain the velocity-independent distribution of s given all the reference events $s_1, \ldots, s_{N_s}$

$$p_{\mathrm{INT}}(s \mid s_1, \ldots, s_{N_s}, \{r_{\alpha,i,*}, \hat{\tau}_{\alpha,i,*}\}) = \sum_{V \in \mathcal{V}} p_{\mathrm{INT}}(s \mid s_1, \ldots, s_{N_s}, \{r_{\alpha,i,*}, \hat{\tau}_{\alpha,i,*}\}, V)\,p(V). \tag{16}$$

To solve eqs (12) and (15) numerically, we approximate the partial derivative with a finite difference

$$\partial_r\tau_\alpha(s_i, s, r_{\alpha,i,*} \mid V) \approx \frac{\tau_\alpha(s_i, s, r_{\alpha,i,*} + \Delta r \mid V) - \tau_\alpha(s_i, s, r_{\alpha,i,*} - \Delta r \mid V)}{2|\Delta r|}, \tag{17}$$

which, as for double-difference, allows us to efficiently compute the posterior distribution in eq. (15) using an eikonal solver for fully 3-D velocity models.

3.4 Comparison of the two location methods

The double-difference and interferometric location methods presented above have advantages and disadvantages. The double-difference location algorithm partially removes the velocity uncertainty by using traveltime differences and significantly reduces the impact of noise by averaging over many receivers thus reducing the spread of the estimator. The interferometric method is even less sensitive to velocity perturbations between the reference sources and the monitoring well when the geometry is suitable as is the case when the velocity is layered and monitoring well is vertical.

To test the performance of both methods we consider the numerical experiment shown in Fig. 1. We assume that the signal, and hence $\hat{T}_{\alpha,i}$ and $\hat{\tau}_{\alpha,i,j}$, are noisy. In addition we also assume that the velocity in the overburden above the events is uncertain. Although our approach can accommodate different forms of velocity uncertainty, for ease of presentation we consider here a simplified uncertainty model in which there is only a single uncertainty parameter. Let $V_{\alpha,0}, \alpha \in \{P, S\}$ be the true velocity models shown in Fig. 1(a). The estimated velocities, $V_\alpha(z)$ are assumed to have the form

$$V_\alpha(z) = V_{\alpha,0}(z)\big(1 + \eta(z)\big), \tag{18}$$

where

$$\eta(z) = \begin{cases} \eta & z < 2500 \\ 0 & z \geq 2500 \end{cases}. \tag{19}$$

This means that the velocities inside the production layer are known exactly, whereas the velocity above that can be overestimated or underestimated by the random factor η. Assuming zero uncertainty in the reservoir layer also allows us to clearly separate the effects of noise and velocity uncertainty in the overburden. We will consider a more general example in the last section of the paper.

We first show the effect of the uncertainty in velocity and the error in the lag time pick on the performance of both methods. Fig. 3 contains the location results for the two methods for a range of η and ζ. The relative velocity error η assumes values -20 per cent, -10 per cent, 0, 10 per cent, 20 per cent, and ζ takes values 4, 2 and 1 ms. Each row in Fig. 3 corresponds to the same velocity error, and each column corresponds to the same ζ. We show the 95 per cent confidence region in the offset-depth domain; the results of the double-difference method are shown in blue, and the results of the interferometric method are shown in green.
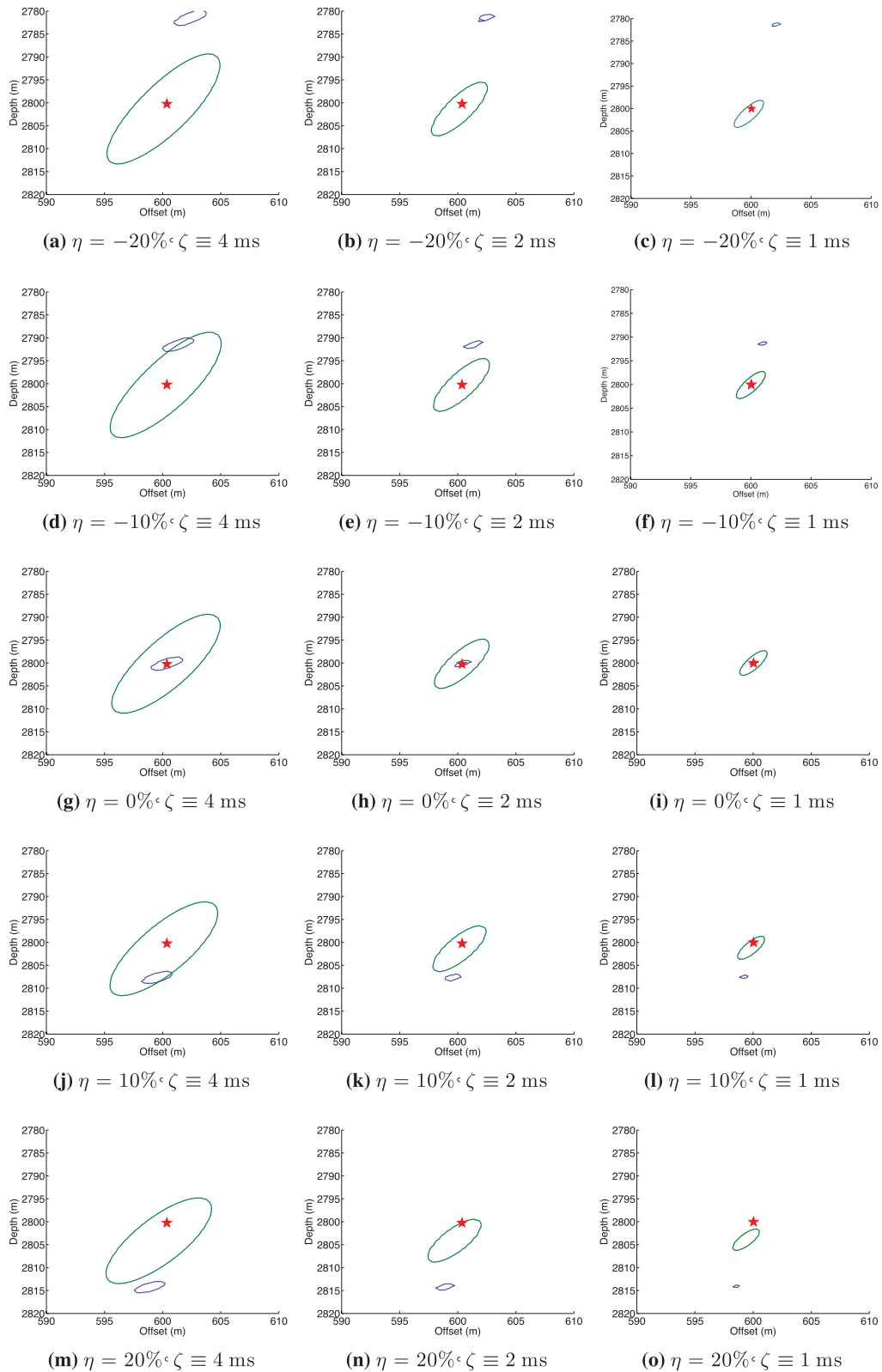
Figure 3. 95 per cent confidence regions for double-difference (blue) and interferometric (green) location using an incorrect velocity model. Results are shown for various choices of overburden velocity perturbation η and signal noise ζ.

(a) $\zeta \equiv 4$ ms   **(b)** $\zeta \equiv 2$ ms   **(c)** $\zeta \equiv 1$ ms
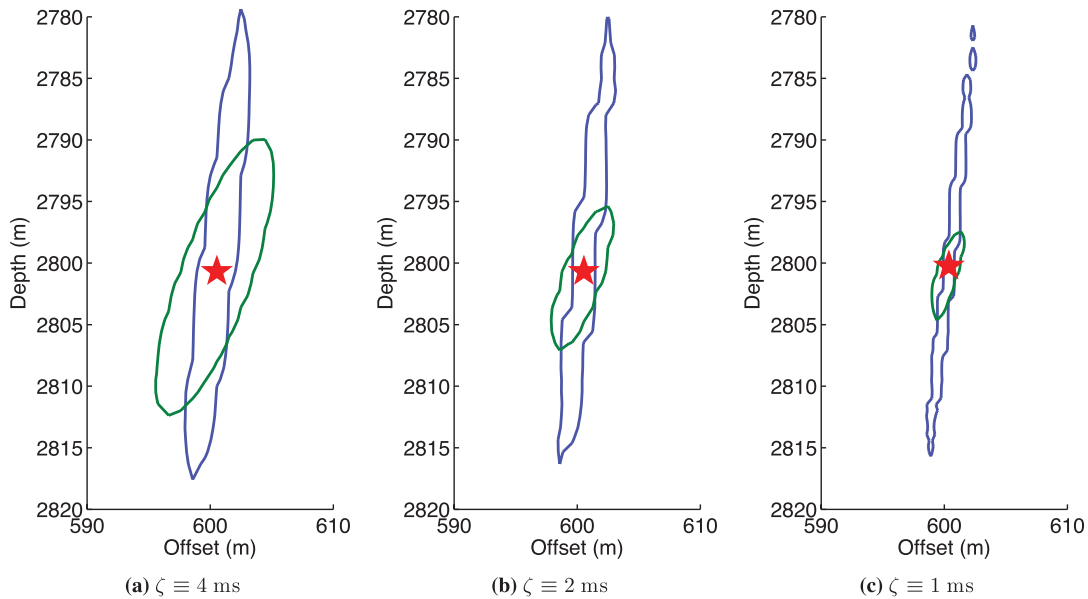
Figure 4. 95 per cent confidence regions for double-difference (blue) and interferometric (green) location averaged over all admissible velocity models. Results are shown for three choices of signal noise ζ.

Evaluating panels from the same row in Fig. 3, we observe that as ζ becomes smaller, so do the uncertainty regions for both methods. The uncertainty region of the double-difference method is always smaller due to averaging over a larger number of measurements.

Examining panels from the same column, we see that varying the velocity error in the overburden leaves the uncertainty produced by the interferometric estimator very stable. This is because the effect of overburden velocity uncertainty is mitigated during the stationary phase analysis (Poliannikov *et al.* 2011). At the same time, the results of the double-difference method show a clear dependence on the velocity error. The larger the error, the more biased the results become.

In practice we cannot know for sure how much the assumed velocity model is different from the true one. The total uncertainty of the estimated location should include velocity uncertainty as spelled out by eqs (11) and (16). For illustration purposes, we will assume that eqs (18) and (19) hold with $\eta \sim \mathcal{N}(0, 10 \text{ per cent})$. We compute the total uncertainty of the event location for different choices of the correlation pick uncertainty and show the results in Fig. 4.

Each of the three panels in Fig. 4 can be loosely thought of as an average (weighted by the Gaussian probabilities) of the respective columns in Fig. 3. The bias that the double-difference method produces for each realization of the velocity model, $V \in \mathcal{V}$, translates into a larger uncertainty region when we compute the total uncertainty by averaging over $\mathcal{V}$. The tortuous shape of the uncertainty region is due to the layered velocity and the specific model for the velocity uncertainty. Different assumptions on the velocity would result in different (generally non-Gaussian) shapes of the uncertainty regions. The artefact in Fig. 4(c) is due to the insufficiently high spatial resolution of the numerical model.

The relative performance of the double-difference location method versus the interferometric location method for this example depends on the noise strength and the velocity uncertainty. When ζ goes to zero, the velocity uncertainty dominates. The interferometric location method, which is better adapted to handle this, is expected to perform better. On the other hand, if the velocity is well resolved then the error due to signal noise dominates. By averaging over a larger number of measurements, the double-difference location method then produces a better estimator.

3.5 Unified Bayesian method

Both location methods presented earlier use the locations of known events to produce estimators of an unknown event location. Both methods derive additional information about the unknown event location from the correlograms by fitting predicted traveltime differences into observed correlations. The difference between the two methods lies in the choice of the norm used for the fitting. The double-difference location method is based on fitting the predicted correlogram events to the observed correlations by using the ℓ_2 norm over all receivers. When the noise in the signal is uncorrelated and Gaussian, this leads to the optimal estimate. The interferometric method attempts to match the predicted and observed correlograms only at the stationary phase point, which, in a suitable geometry, may lead to a better estimator in the case of an uncertain overburden velocity.

The quality of an estimator may be judged by the volume of the uncertainty region for a fixed confidence level once velocity uncertainty has been marginalized away. The method that produces a confidence region smaller than all others is optimal for a given geometry and set of
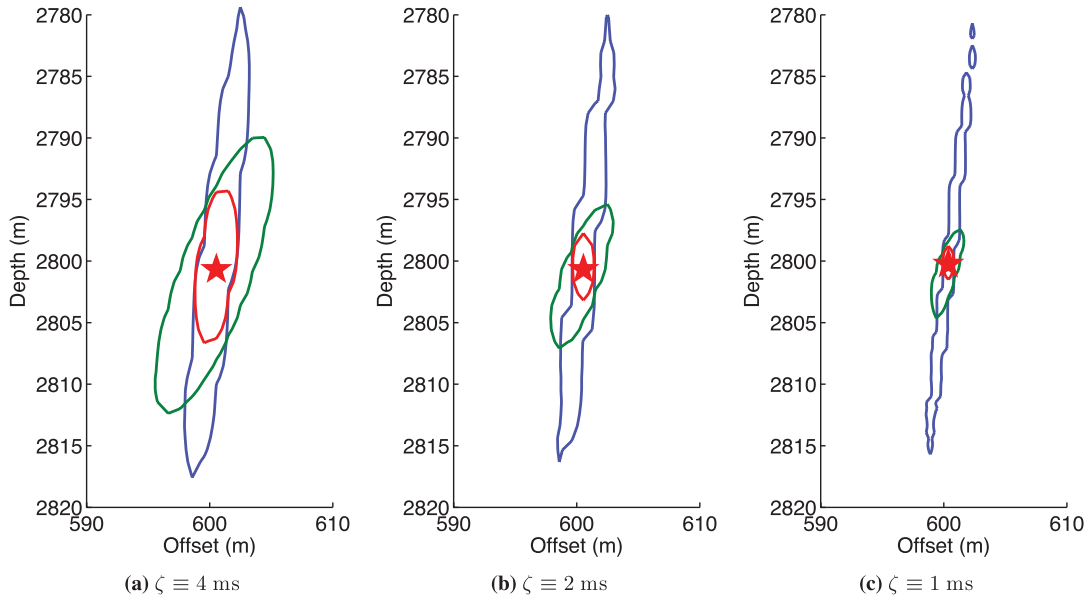
(a) $\zeta \equiv 4$ ms   **(b)** $\zeta \equiv 2$ ms   **(c)** $\zeta \equiv 1$ ms

Figure 5. 95 per cent confidence regions for double-difference (blue), interferometric (green) and unified location (red). Results are shown for three choices of signal noise ζ.

assumptions about uncertainty. We use this simple idea to propose a new unified method of location of one event relative to others. Instead of fitting the data at all receivers equally or fitting it just at the locations of stationary receivers, we assign binary weights, $w_{\alpha,i,j} \in \{0, 1\}$, to each phase α, and each receiver, j, for each reference source, i. The weighted likelihood function has the form

$$p_{\text{BAY}}(\{\hat{\tau}_{\alpha,i,j}\} \mid s, s_1, \ldots, s_{N_s}, V) \propto \exp\left[-\frac{1}{2} \sum_{i=1}^{N_s} \sum_{\alpha,j} w_{\alpha,i,j} \left(\frac{\hat{\tau}_{\alpha,i,j} - \tau_\alpha\left(s_i, s, r_j \mid V\right)}{\zeta_{\alpha,i,j}} \right)^2 \right]. \tag{20}$$

The resulting estimator can be written as

$$p_{\text{BAY}}(s \mid s_1, \ldots, s_{N_s}, \{\hat{\tau}_{\alpha,i,j}\}, V) \propto \frac{p_{\text{BAY}}(\{\hat{\tau}_{\alpha,i,j}\} \mid s, s_1, \ldots, s_{N_s}, V)}{\iiint p_{\text{BAY}}(\{\hat{\tau}_{\alpha,i,j}\} \mid s, s_1, \ldots, s_{N_s}, V)\, ds}, \tag{21}$$

and

$$p_{\text{BAY}}(s \mid s_1, \ldots, s_{N_s}, \{\hat{\tau}_{\alpha,i,j}\}) = \sum_{V \in \mathcal{V}} p_{\text{BAY}}(s \mid s_1, \ldots, s_{N_s}, \{\hat{\tau}_{\alpha,i,j}\}, V)\, p(V). \tag{22}$$

Having constructed the estimator, we can compute the volume, W, of its 95 per cent confidence region. The optimal weights are then found by solving the minimization problem

$$\{w^0_{\alpha,i,j}\} = \arg \min_{\{w_{\alpha,i,j}\}} W. \tag{23}$$

Solving this minimization problem for a large data set and many admissible velocity models is not completely trivial. We illustrate the unified location method by using a slightly simplified optimization procedure organized as follows. For each reference event number i, we seek the connected window of receivers, $\{j, j + 1, \ldots\}$, that minimizes the estimate of the location uncertainty. This greatly reduces the parameter space for the optimization problem, and is likely to be optimal for all examples shown in the paper.

The final results for this model are shown in Fig. 5. The unified method outperforms both the double-difference and the interferometric method by taking the best of both worlds. For each reference source, the algorithm automatically finds a window of receivers centred roughly at the stationary point. The location bias that is introduced by receivers above the stationary depth is approximately removed by the bias from receivers below the stationary location. By combining the contributions of all receivers, we minimize the bias caused by the velocity uncertainty while simultaneously reducing noise by averaging over many receivers.

4 UNKNOWN ORIGIN TIMES

All of the theory presented earlier assumed the knowledge of origin times. Propagation times could be easily inferred from the corresponding event picks, which greatly simplified the analysis. In this section, we show for completeness that knowledge of event origin times is not necessary, and our analysis fully extends to the more realistic case in which the origin times are unknown.

4.1 Classical location in known velocity

Suppose as before that a single event with an unknown hypocentre s is recorded at all receivers. Denoting its origin time $\mathring{T}$, we write the following expression for the event time picks

$$\hat{T}_{\alpha,j} = \mathring{T} + T_\alpha\left(s, r_j\right) + \varepsilon_{\alpha,j}, \quad \alpha = P, S, \dots, \quad j = 1, \dots, N_r, \tag{24}$$

where $\varepsilon_{\alpha,j} \sim \mathcal{N}(0, \sigma_{\alpha,j}^2)$. Note that $\hat{T}_{\alpha,j}$ now refers to time of day (absolute time) instead of its former meaning of traveltime, whereas $T_\alpha(s, r_j)$ retains its meaning of predicted traveltime.

The likelihood function describing the probability of observing specific times given a source location and an origin time has the form

$$p_{\text{CL}}\left(\{\hat{T}_{\alpha,j}\} \mid s, \mathring{T}\right) = \frac{1}{(2\pi)^{N_r/2} \prod_{\alpha,j} \sigma_{\alpha,j}} \exp\left[-\frac{1}{2}\sum_{\alpha,j}\left(\frac{\hat{T}_{\alpha,j} - \mathring{T} - T_\alpha\left(s, r_j\right)}{\sigma_{\alpha,j}}\right)^2\right]. \tag{25}$$

The posterior joint distribution of the event's location and origin time given the observed time picks is again obtained by Bayes' theorem

$$p_{\text{CL}}\left(s, \mathring{T} \mid \{\hat{T}_{\alpha,j}\}\right) = \frac{p_{\text{CL}}\left(\{\hat{T}_{\alpha,j}\} \mid s, \mathring{T}\right) p(s, \mathring{T})}{\int\int p_{\text{CL}}\left(\{\hat{T}_{\alpha,j}\} \mid s, \mathring{T}\right) p(s, \mathring{T})\, d\mathring{T}\, ds}. \tag{26}$$

The prior distribution, $p(s, \mathring{T})$, reflects our very limited understanding of the event origin times and locations in the absence of any recorded data. We assume a uniform distribution $p(s, \mathring{T}) \equiv \text{const}$ on a sufficiently large spatial volume and temporal interval. The likelihood function, $p_{\text{CL}}(\{\hat{T}_{\alpha,j}\} \mid s, \mathring{T})$, is given above, and it captures the physics of wave propagation between event locations and receivers. Scenarios incompatible with recorded data, such as the event occurring after it is recorded by the receivers, will be automatically ruled out by the likelihood function during the computation of the posterior distribution, $p_{\text{CL}}(s, \mathring{T} \mid \{\hat{T}_{\alpha,j}\})$.

Under the assumption of a uniform prior distribution, the posterior distribution adopts the compact form

$$p_{\text{CL}}\left(s, \mathring{T} \mid \{\hat{T}_{\alpha,j}\}\right) \propto \exp\left[-\frac{1}{2}\sum_{\alpha,j}\left(\frac{\hat{T}_{\alpha,j} - \mathring{T} - T_\alpha\left(s, r_j\right)}{\sigma_{\alpha,j}}\right)^2\right]. \tag{27}$$

Eq. (27) for the posterior distribution of the event location and origin time captures both the spatial and temporal uncertainty about the event as well as the correlation between the two. This information could potentially be used to track the microseismic activity as a function of time. If we are interested only in the spatial uncertainty of the event then that can be obtained by marginalizing away the origin time:

$$p_{\text{CL}}\left(s \mid \{\hat{T}_{\alpha,j}\}\right) \propto \int p_{\text{CL}}\left(s, \mathring{T} \mid \{\hat{T}_{\alpha,j}\}\right) d\mathring{T} = \int \exp\left[-A\mathring{T}^2 - B\mathring{T} - C\right] d\mathring{T} \propto \exp\left[\frac{B^2}{4A} - C\right], \tag{28}$$

where

$$A = \frac{1}{2}\sum_{\alpha,j}\frac{1}{\sigma_{\alpha,j}^2},$$

$$B = -\sum_{\alpha,j}\frac{\hat{T}_{\alpha,j} - T_\alpha\left(s, r_j\right)}{\sigma_{\alpha,j}^2},$$

$$C = \frac{1}{2}\sum_{\alpha,j}\frac{\left(\hat{T}_{\alpha,j} - T_\alpha\left(s, r_j\right)\right)^2}{\sigma_{\alpha,j}^2}. \tag{29}$$

4.2 Relative location in uncertain velocity

Assume as before that the reference events, $s_1, \dots, s_{N_s}$, have already been located. The measured traveltime difference between the two direct arrivals from events s and s_i has the form

$$\hat{\tau}_{\alpha,i,j} = \tau_\alpha\left(s_i, s, r_j \mid V\right) + \mathring{T} - \mathring{T}_i + \eta_{\alpha,i,j}, \tag{30}$$

where $\tau_\alpha(s_i, s, r_j \mid V) = T_\alpha(s, r_j \mid V) - T_\alpha(s_i, r_j \mid V)$, $\mathring{T}$ is the origin time of the unknown event, s, and $\mathring{T}_i$ are the origin times of the reference events, s_i. For convenience we define the unknown differences of the origin times $\Delta\mathring{T}_i = \mathring{T} - \mathring{T}_i, i = 1, \dots, N_s$, and show how they affect the location uncertainty for each method of relative location discussed so far.

4.2.1 Double-difference

The posterior distribution of $\mathbf{s}$ with origin times accounted for is written as

$$p_{\mathrm{DD}}(\mathbf{s} \mid \mathbf{s}_1, \ldots, \mathbf{s}_{N_s}, \{\hat{\tau}_{\alpha,i,j}\}, V) \propto \prod_{i=1}^{N_s} \exp\left[\frac{B_i^2}{4A_i} - C_i\right], \qquad (31)$$

where

$$A_i = \frac{1}{2}\sum_{\alpha,j} \frac{1}{\zeta_{\alpha,i,j}^2},$$

$$B_i = -\sum_{\alpha,j} \frac{\hat{\tau}_{\alpha,i,j} - \tau_\alpha\left(\mathbf{s}_i, \mathbf{s}, \mathbf{r}_j \mid V\right)}{\zeta_{\alpha,i,j}^2},$$

$$C_i = \frac{1}{2}\sum_{\alpha,j} \frac{\left(\hat{\tau}_{\alpha,i,j} - \tau_\alpha\left(\mathbf{s}_i, \mathbf{s}, \mathbf{r}_j \mid V\right)\right)^2}{\zeta_{\alpha,i,j}^2}. \qquad (32)$$

This result is derived in the Appendix in Section A1. By averaging over all possible velocity realizations we obtain a velocity independent double-difference estimator of the event location:

$$p_{\mathrm{DD}}(\mathbf{s} \mid \mathbf{s}_1, \ldots, \mathbf{s}_{N_s}, \{\hat{\tau}_{\alpha,i,j}\}) = \sum_{V \in \mathscr{V}} p_{\mathrm{DD}}(\mathbf{s} \mid \mathbf{s}_1, \ldots, \mathbf{s}_{N_s}, \{\hat{\tau}_{\alpha,i,j}\}, V)\, p(V). \qquad (33)$$

4.2.2 Interferometric location

For the interferometric likelihood function with arbitrary origin times, we have

$$p_{\mathrm{INT}}(\mathbf{s} \mid \mathbf{s}_1, \ldots, \mathbf{s}_{N_s}, \{\mathbf{r}_{\alpha,i,*}, \hat{\tau}_{\alpha,i,*}\}, V) \propto \prod_{i=1}^{N_s} \exp\left[\frac{B_i^2}{4A_i} - C_i\right], \qquad (34)$$

where now

$$A_i = \sum_\alpha \frac{1}{2\zeta_{\alpha,i,*}^2},$$

$$B_i = -\sum_\alpha \frac{\hat{\tau}_{\alpha,i,*} - \tau_\alpha\left(\mathbf{s}_i, \mathbf{s}, \mathbf{r}_{\alpha,i,*} \mid V\right)}{\zeta_{\alpha,i,*}^2},$$

$$C_i = \sum_\alpha \left[\frac{\left(\hat{\tau}_{\alpha,i,*} - \tau_\alpha\left(\mathbf{s}_i, \mathbf{s}, \mathbf{r}_{\alpha,i,*} \mid V\right)\right)^2}{2\zeta_{\alpha,i,*}^2} + \frac{\partial_r \tau_\alpha\left(\mathbf{s}_i, \mathbf{s}, \mathbf{r}_{\alpha,i,*} \mid V\right)}{8\zeta_{\alpha,i,*}^2}\right]. \qquad (35)$$

This result is derived in the Appendix in Section A2. Averaging over different velocity uncertainties, we obtain

$$p_{\mathrm{INT}}(\mathbf{s} \mid \mathbf{s}_1, \ldots, \mathbf{s}_{N_s}, \{\mathbf{r}_{\alpha,i,*}, \hat{\tau}_{\alpha,i,*}\}) = \sum_{V \in \mathscr{V}} p_{\mathrm{INT}}(\mathbf{s} \mid \mathbf{s}_1, \ldots, \mathbf{s}_{N_s}, \{\mathbf{r}_{\alpha,i,*}, \hat{\tau}_{\alpha,i,*}\}, V)\, p(V). \qquad (36)$$

4.2.3 Unified Bayesian method

The formulas for the likelihood function and the posterior distribution for the unified method are notationally identical to those for the double-difference method. The only difference is that the summations $\sum_{\alpha,i,j}$ are performed only over triplets (α, i, j), for which the weights $w_{\alpha,i,j}$ are nonzero.

4.3 Numerical results

The 95 per cent uncertainty regions for all three methods are shown in Fig. 6. Qualitatively they are very similar to the case of known origin times. We can see that due to a larger number of constraints used to build the estimator, the double-difference method better handles the uncertainty in the origin times than the interferometric method. The unified method as before outperforms both the double-difference and the interferometric methods.

5 MORE GENERAL VELOCITY MODELS

We have presented a unified method of relative location of seismic events. Given an explicitly given set of assumption about the velocity uncertainty and signal noise, we can select the best receivers that minimize the location uncertainty. In many practical cases the production
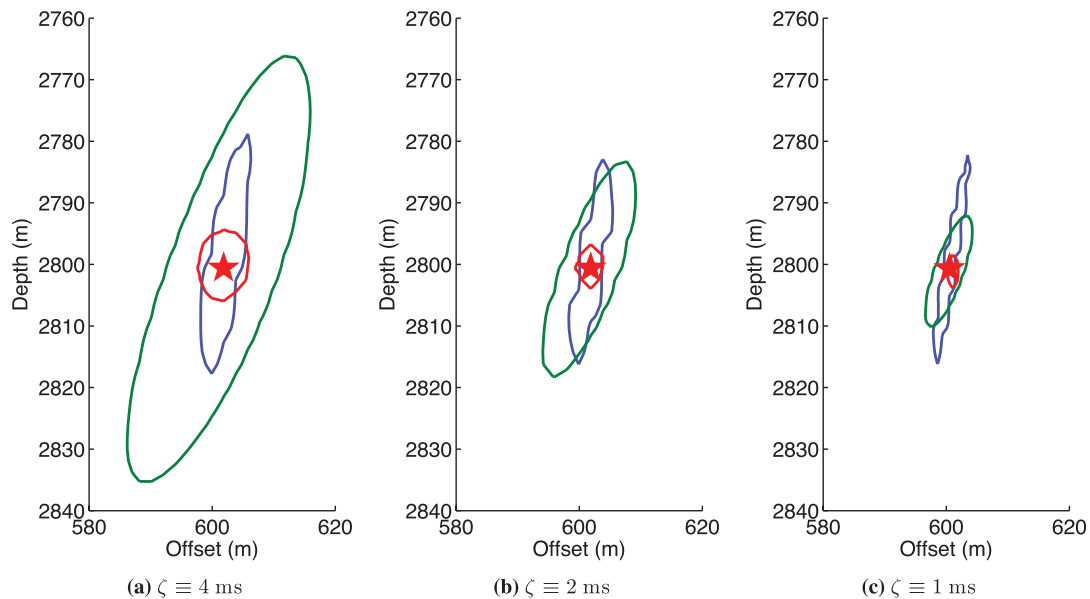
Figure 6. 95 per cent confidence regions for double-difference (blue), interferometric (green) and unified location (red) with unknown origin times. Results are shown for three choices of signal noise ζ.

layer is known better due to the availability of horizontal wells in the production layer, well logs and the better ray coverage by perforation shots. We have demonstrated the power of our relative location method in this type of situation.

The formulas that govern all of the location methods presented above are general. They do not require assumptions about a specific form of the velocity uncertainty or well geometry. Here, we show numerical results of applying our methodology to other realistic scenarios. The list of setups is not exhaustive; it simply confirms the inherent versatility of our approach.

We generalize the familiar numerical setup in two ways. First, we assume that the velocity inside the production layer is also uncertain. Secondly, we allow the velocity inside each layer to vary horizontally as well as vertically. Specifically, we suppose that the mean velocity inside each layer is as before. The assumed velocity is the sum of the mean velocity and a realization of a Gaussian random field with zero mean. The standard deviation of random perturbations is 10 per cent in the overburden, and it varies from 1 to 10 per cent in the production layer. We will thus consider a range of scenarios from the one where the production layer uncertainty is small to one where the uncertainty in the production layer is as large as it is in the overburden. The correlation length of random velocity perturbations is fixed at 100 m in the vertical direction, and it varies from 100 m to 5 km in the horizontal direction. We assume throughout this section that the standard deviation of the error in time picks is 1 ms.

Fig. 7 shows typical velocity realizations for each setup, optimal receivers obtained by the hybrid method and the resulting minimal uncertainty. Elliptical approximations are used to display the confidence regions, to save computation time. For these more complicated models many velocity realizations are needed to obtain a smooth curve, but good elliptical approximations can be made with relatively few realizations. We can see that when the uncertainty inside the production layer is small, near-stationary receivers produce the smallest uncertainty. This is in agreement with previous results for the fully known production layer. When the uncertainty inside the production layer becomes larger, using only the nearly stationary receivers presents no advantage. Consequently, it appears in this case best to simply use more receivers to reduce the effects of velocity uncertainty and signal noise.

The horizontal correlation length of the velocity uncertainty also affects the optimization result. When the horizontal length is small, rays that connect the same shallow receiver to different sources travel through uncorrelated parts of the medium, and errors in traveltime do not cancel during cross-correlation. Including these receivers in the likelihood function adds noise and increases uncertainty. As the horizontal correlation length increases, the situation changes. The correlation between errors in traveltime along different rays increases, and thus these errors are cancelled by cross-correlation. Including shallow receivers in this case helps minimize location uncertainty. In the extreme case, where correlation is long and the model takes on a more finely layered structure, and the velocity uncertainty in the overburden and the production layer are equally large, only shallow receivers are useful. Traveltimes along the rays from near-stationary receivers to the events have the largest errors, and thus these receivers are best left unused.

The analysis presented above serves as an illustration of the power of the proposed methodology of finding the best relative location algorithm in various situations. The conclusions drawn in this section are model specific and do not extend to other geometries; however, the overall methodology does.

6 CONCLUSIONS

In this paper, we propose a unified framework for locating an unknown event relative to other known events. This problem is pervasive in hydrofracture monitoring where we seek to describe the position of one fracture relative to another. We have analysed two methods for event
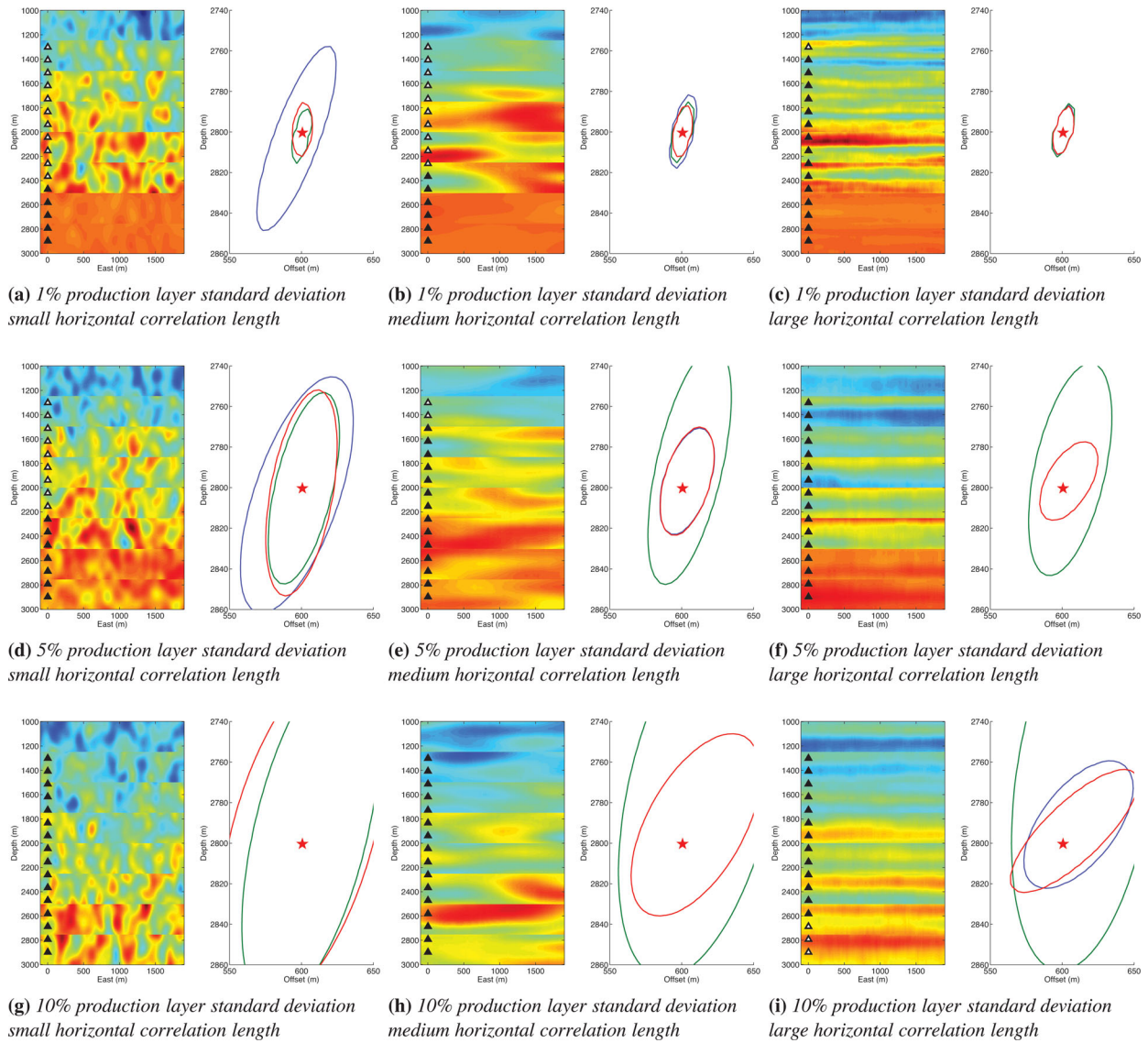
(a) *1% production layer standard deviation small horizontal correlation length*

(b) *1% production layer standard deviation medium horizontal correlation length*

(c) *1% production layer standard deviation large horizontal correlation length*

(d) *5% production layer standard deviation small horizontal correlation length*

(e) *5% production layer standard deviation medium horizontal correlation length*

(f) *5% production layer standard deviation large horizontal correlation length*

(g) *10% production layer standard deviation small horizontal correlation length*

(h) *10% production layer standard deviation medium horizontal correlation length*

(i) *10% production layer standard deviation large horizontal correlation length*

Figure 7. Elliptical approximations of 95 per cent confidence regions for double-difference (blue), interferometric (green) and hybrid (red) location. Results are shown for various strengths of velocity perturbations inside the production layer, and for various correlation lengths throughout the model. The signal noise is fixed at 1 ms for all panels. Typical velocity realizations are shown on the left. Black triangles denote optimal receivers found during optimization.

location, double-difference and interferometry, and compared them in numerical experiments with receivers in a vertical monitoring well. We have shown that each of them is well-suited for specific assumptions about the geometry of the experiment, the signal noise and the uncertainty in the velocity model. In our experiment the double-difference method handles the noise in the signal well, and it reduces the effect of the velocity uncertainty. The interferometric location method is even better at mitigating the velocity uncertainty in the overburden, but it is less able to deal with the noise in lag picks.

To deal with a full range of uncertainty scenarios, both in the velocity and in the recorded signal, we have proposed a unified location method. This algorithm incorporates the best properties of double-difference and interferometry by selectively using data so as to minimize the uncertainty of event locations.

ACKNOWLEDGEMENTS

REFERENCES

Bennett, L. *et al.*, 2005. The source for hydraulic fracture characterization, *Oilfield Rev.,* **17**(4), 42–57.

Borcea, L., Papanicolaou, G. & Tsogka, C., 2005. Interferometric array imaging in clutter, *Inv. Probl.,* **21,** 1419–1460.

Dewey, J., 1972. Seismicity and tectonics of Western Venezuela, *Bull. seism. Soc. Am.,* **62,** 1711–1751.

Eisner, L., Fischer, T. & Calvez, J.H.L., 2006. Detection of repeated hydraulic fracturing (out-of-zone growth) by microseismic monitoring. *Leading Edge,* **25,** 548–554.

Eisner, L., Hulsey, B.J., Duncan, P., Jurick, D., Werner, H. & Keller, W., 2010. Comparison of surface and borehole locations of induced seismicity, *Geophys. Prospect.,* **58**(5), 809–820.

Fitch, T., 1975. Compressional velocity in source regions of deep earthquakes: an application of the master earthquake technique, *Earth planet. Sci. Lett.,* **26,** 156–166.

Huang, Y.A., Chen, J. & Benesty, J., 2006. Time delay estimation and acoustic source localization, in *Acoustic MIMO Signal Processing,* pp. 215–259, eds Huang, Y.A., Benesty, J. & Chen, J., Signals and Communication Technology—Springer, US.

Hulsey, B.J., Eisner, L., Thornton, M. & Jurick, D., 2009. Application of relative location technique from surface arrays to microseismicity induced by shale fracturing. *Expanded Abstr.,* **28,** 1602–1606.

Kummerow, J., 2010. Using the value of the crosscorrelation coefficient to locate microseismic events, *Geophysics,* **75**(4), MA47–MA52.

Michaud, G., Leslie, D., Drew, J., Endo, T. & Tezuka, K., 2004. Microseismic event localization and characterization in a limited aperture HFM experiment. *SEG Expanded Abstr.,* **23,** 552–555.

Michelini, A. & Lomax, A., 2004. The effect of velocity structure errors on double-difference earthquake location, *Geophys. Res. Lett.,* **31,** L09602, doi:10.1029/2004GL019682.

Pavlis, G.L., 1986. Appraising earthquake hypocenter location errors: a complete, practical approach for single-event locations, *Bull. seism. Soc. Am.,* **76**(6), 1699–1717.

Poliannikov, O.V., Malcolm, A.E., Djikpesse, H. & Prange, M., 2011. Interferometric hydrofracture microseism localization using neighboring fracture, *Geophysics,* **76**(6), WC27–WC36.

Richards, P. G., Waldhauser, F., Schaff, D. & Kim, W.-Y., 2006. The applicability of modern methods of earthquake location, *Pure appl. Geophys.,* **163,** 351–372.

Spence, W., 1980. Relative epicenter determination using P-wave arrival-time differences, *Bull. seism. Soc. Am.,* **70,** 171–183.

Tarantola, A. & Valette, B., 1982. Inverse problems = quest for information, *J. Geophys.,* **50,** 159–170.

Waldhauser, F. & Ellsworth, W.L., 2000. A double-difference earthquake location algorithm: method and application to the Northern Hayward Fault, California, *Bull. seism. Soc. Am.,* **90**(6), 1353–1368.

Zhang, H. & Thurber, C.H., 2003. Double-difference tomography: the method and its application to the Hayward Fault, California, *Bull. seism. Soc. Am.,* **93**(5), 1875–1889.

Zhang, H. & Thurber, C.H., 2006. Development and applications of double-difference seismic tomography, *Pure appl. Geophys.,* **163,** 373–403.

APPENDIX A: POSTERIOR DISTRIBUTIONS FOR RELATIVE LOCATION METHODS

A1 Posterior distribution for double-difference

Adding the unknown event origin times leads to the following form of the likelihood function:

$$p_{DD}(\{\hat{\tau}_{\alpha,i,j}\} \mid s, \Delta\mathring{T}_1, \dots, \Delta\mathring{T}_{N_s}, s_1, \dots, s_{N_s}, V) \propto \exp\left[-\frac{1}{2} \sum_{i=1}^{N_s} \sum_{\alpha,j} \left(\frac{\hat{\tau}_{\alpha,i,j} - \tau_\alpha\left(s_i, s, r_j \mid V\right) - \Delta\mathring{T}_i}{\zeta_{\alpha,i,j}} \right)^2 \right]. \tag{A1}$$

Applying Bayes' rule and assuming that $p(s, \Delta\mathring{T}_1, \dots \Delta\mathring{T}_{N_s}) \equiv$ const, we obtain

$$p_{DD}(s, \Delta\mathring{T}_1, \dots, \Delta\mathring{T}_{N_s} \mid s_1, \dots, s_{N_s}, \{\hat{\tau}_{\alpha,i,j}\}, V) \propto \frac{p_{DD}(\{\hat{\tau}_{\alpha,i,j}\} \mid s, \Delta\mathring{T}_1, \dots, \Delta\mathring{T}_{N_s}, s_1, \dots, s_{N_s}, V)}{\int \dots \int p_{DD}(\{\hat{\tau}_{\alpha,i,j}\} \mid s, \Delta\mathring{T}_1, \dots, \Delta\mathring{T}_{N_s}, s_1, \dots, s_{N_s}, V) \, d\Delta\mathring{T}_1 \cdots d\Delta\mathring{T}_{N_s} \, ds}. \tag{A2}$$

The posterior distribution of s is written as:

$$p_{DD}(s \mid s_1, \dots, s_{N_s}, \{\hat{\tau}_{\alpha,i,j}\}, V) = \int \dots \int p_{DD}(s, \Delta\mathring{T}_1, \dots, \Delta\mathring{T}_{N_s}, \mid s_1, \dots, s_{N_s}, \{\hat{\tau}_{\alpha,i,j}\}, V) \, d\Delta\mathring{T}_1 \cdots d\Delta\mathring{T}_{N_s}$$

$$= \frac{\int \dots \int p_{DD}(\{\hat{\tau}_{\alpha,i,j}\} \mid s, \Delta\mathring{T}_1, \dots, \Delta\mathring{T}_{N_s}, s_1, \dots, s_{N_s}, V) \, d\Delta\mathring{T}_1 \cdots d\Delta\mathring{T}_{N_s}}{\int \int \dots \int p_{DD}(\{\hat{\tau}_{\alpha,i,j}\} \mid s, \Delta\mathring{T}_1, \dots, \Delta\mathring{T}_{N_s}, s_1, \dots, s_{N_s}, V) \, d\Delta\mathring{T}_1 \cdots d\Delta\mathring{T}_{N_s} ds}. \tag{A3}$$

The multidimensional integral over $\Delta\mathring{T}_1, \dots, \Delta\mathring{T}_{N_s}$ in the numerator and the denominator of the right hand side of the last equation can be again computed analytically. Indeed, we have

$$\int \dots \int p_{DD}(\{\hat{\tau}_{\alpha,i,j}\} \mid s, \Delta\mathring{T}_1, \dots, \Delta\mathring{T}_{N_s}, s_1, \dots, s_{N_s}, V) \, d\Delta\mathring{T}_1 \cdots d\Delta\mathring{T}_{N_s} = \prod_{i=1}^{N_s} \int \exp\left[-\frac{1}{2} \sum_{\alpha,j} \left(\frac{\hat{\tau}_{\alpha,i,j} - \tau_\alpha\left(s_i, s, r_j \mid V\right) - \Delta\mathring{T}_i}{\zeta_{\alpha,i,j}} \right)^2 \right] d\Delta\mathring{T}_i$$

$$= \prod_{i=1}^{N_s} \int \exp\left[-A_i \Delta\mathring{T}_i^2 - B_i \Delta\mathring{T}_i - C_i \right] d\Delta\mathring{T}_i$$

$$= \prod_{i=1}^{N_s} \sqrt{\frac{\pi}{A_i}} \exp\left[\frac{B_i^2}{4 A_i} - C_i \right], \tag{A4}$$

where

$$A_i = \frac{1}{2} \sum_{\alpha, j} \frac{1}{\zeta_{\alpha, i, j}^2},$$

$$B_i = -\sum_{\alpha, j} \frac{\hat{\tau}_{\alpha, i, j} - \tau_\alpha \left(s_i, s, r_j \mid V \right)}{\zeta_{\alpha, i, j}^2},$$

$$C_i = \frac{1}{2} \sum_{\alpha, j} \frac{\left(\hat{\tau}_{\alpha, i, j} - \tau_\alpha \left(s_i, s, r_j \mid V \right) \right)^2}{\zeta_{\alpha, i, j}^2}. \tag{A5}$$

A2 Posterior distribution for interferometric location

For the interferometric likelihood function, we have

$$p_{\text{INT}}(\{r_{\alpha, i, *}, \hat{\tau}_{\alpha, i, *}\} \mid s, \Delta \mathring{T}_1, \ldots, \Delta \mathring{T}_{N_s}, s_1, \ldots, s_{N_s}, V) \propto \exp \left[-\frac{1}{2} \sum_{i=1}^{N_s} \sum_\alpha \left(\frac{\hat{\tau}_{\alpha, i, *} - \tau_\alpha \left(s_i, s, r_{\alpha, i, *} \mid V \right) - \Delta \mathring{T}_i}{\zeta_{\alpha, i, *}} \right)^2 \right]$$

$$\times \exp \left[-\frac{1}{2} \sum_{i=1}^{N_s} \sum_\alpha \left(\frac{\partial_r \tau_\alpha \left(s_i, s, r_{\alpha, i, *} \mid V \right)}{2 \zeta_{\alpha, i, *}} \right)^2 \right]. \tag{A6}$$

Following the standard logic, we write the posterior estimator as follows

$$p_{\text{INT}}(s \mid s_1, \ldots, s_{N_s}, \{r_{\alpha, i, *}, \hat{\tau}_{\alpha, i, *}\}, V) \propto \frac{\int \cdots \int p_{\text{INT}}(\{r_{\alpha, i, *}, \hat{\tau}_{\alpha, i, *}\} \mid s, \Delta \mathring{T}_1, \ldots, \Delta \mathring{T}_{N_s}, s_1, \ldots, s_{N_s}, V) d \mathring{T}_1 \cdots d \mathring{T}_{N_s}}{\int \int \cdots \int p_{\text{INT}}(\{r_{\alpha, i, *}, \hat{\tau}_{\alpha, i, *}\} \mid s, \Delta \mathring{T}_1, \ldots, \Delta \mathring{T}_{N_s}, s_1, \ldots, s_{N_s}, V) d \mathring{T}_1 \cdots d \mathring{T}_{N_s} ds}, \tag{A7}$$

where

$$\int \cdots \int p_{\text{INT}}(\{r_{\alpha, i, *}, \hat{\tau}_{\alpha, i, *}\} \mid s, \Delta \mathring{T}_1, \ldots, \Delta \mathring{T}_{N_s}, s_1, \ldots, s_{N_s}, V) d \mathring{T}_1 \cdots d \mathring{T}_{N_s} = \prod_{i=1}^{N_s} \sqrt{\frac{\pi}{A_i}} \exp \left[\frac{B_i^2}{4 A_i} - C_i \right], \tag{A8}$$

and

$$A_i = \sum_\alpha \frac{1}{2 \zeta_{\alpha, i, *}^2},$$

$$B_i = -\sum_\alpha \frac{\hat{\tau}_{\alpha, i, *} - \tau_\alpha \left(s_i, s, r_{\alpha, i, *} \mid V \right)}{\zeta_{\alpha, i, *}^2},$$

$$C_i = \sum_\alpha \left[\frac{\left(\hat{\tau}_{\alpha, i, *} - \tau_\alpha \left(s_i, s, r_{\alpha, i, *} \mid V \right) \right)^2}{2 \zeta_{\alpha, i, *}^2} + \frac{\partial_r \tau_\alpha \left(s_i, s, r_{\alpha, i, *} \mid V \right)}{8 \zeta_{\alpha, i, *}^2} \right]. \tag{A9}$$